
HYDRODYNAMIC APPROACH TO GRAIN CHARGING IN WEAKLY IONIZED PLASMAS¹

L.G. D'YACHKOV, S.A. KHRAPAK¹, A.G. KHRAPAK

UDC 533.9

©2008

Joint Institute for High Temperatures, Russian Academy of Sciences
(Moscow 125412, Russia; e-mail: dyachk@mail.ru and khrapak@mail.ru)

¹**Max-Planck-Institut für extraterrestrische Physik**
(Garching D-85741, Germany; e-mail: skhrapak@mpe.mpg.de)

Influence of the presence of a collisionless (Knudsen) layer around a dust grain in plasma and the electron emission from the grain surface on its charge and screening are investigated. It is assumed that no ionization and recombination occur in the vicinity of the grain. The criterion of the grain charge sign change is obtained. It is shown that, at asymptotically large distances, the electrostatic potential behaves as the Coulomb one with effective charge Z_{eff} which is always negative independently of the sign of the actual charge Z_d . Hence, for $Z_d > 0$, the electrostatic potential changes sign and has a minimum. This indicates the possibility of the existence of the electrostatic attraction between positively charged dust particles.

1. Introduction

The grain charge is one of the most important characteristics of complex (dusty) plasmas which influences many properties of these systems. When the electron/ion emission from the grain surface is absent or small, the grains are negatively charged as a result of the higher mobility of electrons in comparison with that of positive ions [1, 2]. The charge absolute magnitude increases until the flux of ions which are attracted to the grain balances the flux of electrons which are repelled. The electron emission from the grain surface (thermionic, secondary, or photoelectron emission) leads to a decrease of the absolute magnitude of the charge. For a high emission intensity, the charge can even become positive.

Most of the experiments dealing with investigations of ordered structures in complex plasmas have been performed in low-pressure gas discharges. Under these conditions, the ion (electron) mean free path $\ell_{i(e)}$ usually exceeds the characteristic length scale of the perturbed plasma around a grain which is, in the first approximation, of the order of the plasma screening length, λ_D . On this basis, the collisionless orbit motion limited (OML) theory is often used, although the recent

theoretical and experimental results have demonstrated that the charging is considerably influenced by ion-neutral collisions even when ℓ_i is larger than λ_D [2, 3]. In the opposite limiting case of high collisionality $\ell_{i(e)} \ll \lambda_D$, the hydrodynamic approximation can be used.

In the hydrodynamic approximation, it is usually supposed that the grain surface is fully absorbing, and the corresponding zero boundary conditions for the ion and electron densities at the grain surface are used, $n_i(a) = n_e(a) = 0$, where a is the grain radius. However, the application of the hydrodynamic equations down to the grain surface is valid only if the collisionless layer is thin enough relative to the grain size, i.e., when $\ell_{i(e)} \ll a$. But if $\ell_{i(e)} > a$, the presence of the collisionless layer around the grain should be taken into account. There is a wide region of plasma parameters, where this inequality is realized. In [4–6], the zero boundary conditions were modified by the addition of a term comprising the derivative $d[n_{i(e)}r]/dr$. This improves the accuracy of the boundary condition, but still requires $\ell_{i(e)} < a$ to be satisfied.

The purpose of the present paper is to investigate the influence of a collisionless (Knudsen) layer between the grain surface and the surrounding plasma, as well as the electron emission from its surface, on the grain charging and screening processes. We consider a small individual charged grain immersed in the collisional isotropic plasma and neglect the volume ionization and recombination processes. The latter assumption means that plasma sources which compensate for the electron-ion recombination on the grain surface are far from the grain, outside of the plasma perturbed region. The problem of the grain charging under similar conditions but neglecting the Knudsen layer and the electron emission from the grain was investigated in [7].

In this paper, the region $a < r < a + \ell_{i(e)}$ around the grain is approximated by a collisionless layer, while we

¹The results of the work were reported at the 2nd International Conference “Dusty Plasmas in Applications” (August 26–30, 2007, Odessa, Ukraine).

use the drift-diffusion approximation in the outer region $r > a + \ell_{i(e)}$. The approximate algebraic equations for the ion and electron fluxes to the grain and for the grain charge are obtained, and the asymptotic behavior of the electrostatic potential around the grain and its screening are determined.

2. Asymptotic Model of Charging

When the ionization and recombination in the vicinity of the grain are neglected, the total ion (electron) flux that the grain collects (emits) from (to) the surrounding plasma is considered. With regard for the spherical symmetry, we get, in the drift-diffusion approximation (see, e.g., [8]),

$$\frac{dn_{i(e)}}{dr} \pm \frac{en_{i(e)}}{T_{i(e)}} \frac{d\varphi}{dr} = \frac{I_{i(e)}}{4\pi D_{i(e)} r^2}, \quad (1)$$

where $T_{i(e)}$, $D_{i(e)}$, and $I_{i(e)}$ are the ion (electron) temperature (in energy units), diffusion coefficient, and flux to the grain (integration constant), respectively; φ is the electrostatic potential; and the upper (lower) sign corresponds to ions (electrons). Under the stationary conditions $I_i = I_e$, where I_i is the ion flux from the plasma to the grain surface, while I_e is the total electron flux which includes the electron flux from the plasma I_{ep} and the electron emission flux I_{em} (if the latter is present), $I_e = I_{ep} - I_{em}$. The general solutions of Eqs. (1) can be written in the form

$$\begin{aligned} n_{i(e)}(r) = & \exp\left(\mp \frac{e\varphi(r)}{T_{i(e)}}\right) \times \\ & \times \left[n_{i(e)}(r_0) \exp\left(\pm \frac{e\varphi(r_0)}{T_{i(e)}}\right) + \right. \\ & \left. + \frac{I_{i(e)}}{4\pi D_{i(e)}} \int_{r_0}^r \exp\left(\pm \frac{e\varphi(r')}{T_{i(e)}}\right) \frac{dr'}{r'^2} \right], \end{aligned} \quad (2)$$

where r_0 is an arbitrary radius. Usually, r_0 is the radius, at which the boundary conditions are set. If $r_0 \ll \lambda_D$, there is a region $r < r_1$ where the screening is negligible, and the potential can be approximated by the Coulomb form

$$\varphi(r) \cong \frac{eZ_d}{r} + \varphi_c, \quad (3)$$

where Z_d is the grain charge number and φ_c is a certain constant which appears due to the plasma screening of

the grain charge at $r > r_1$ (in vacuum $\varphi_c = 0$). For $r < r_1$, by substituting Eq. (3) into Eqs. (2), we get

$$\begin{aligned} n_i(r) = & \left[n_i(r_0) + \frac{I_i}{4\pi za\tau D_i} \right] \exp\left[z\tau a\left(\frac{1}{r_0} - \frac{1}{r}\right)\right] - \\ & - \frac{I_i}{4\pi za\tau D_i} \end{aligned} \quad (4)$$

$$\begin{aligned} n_e(r) = & \left[n_e(r_0) - \frac{I_e}{4\pi zaD_e} \right] \exp\left[-za\left(\frac{1}{r_0} - \frac{1}{r}\right)\right] + \\ & + \frac{I_e}{4\pi zaD_e}, \end{aligned} \quad (5)$$

where $z = e^2 Z_d / (T_e a)$ is the dimensionless grain charge, and $\tau = T_e / T_i$ is the electron-to-ion temperature ratio. It follows from Eqs. (4) and (5) that, due to the exponential dependence on r , $n_{i(e)}$ quickly approach almost constant values which are very weakly dependent on r . They should be associated with the unperturbed plasma density n_0 . Conditions, under which $n_{i(e)}$ approach the unperturbed level n_0 for plasma particles attracted by the grain, are $r_0 \ll r < r_1$. For repulsed particles, they are $z\tau a \ll r < r_1$ for ions and $za \ll r < r_1$ for electrons. Then Eqs. (4) and (5) are reduced to

$$n_i(r_0) e^{\frac{z\tau a}{r_0}} + \frac{I_i}{4\pi za\tau D_i} (e^{\frac{z\tau a}{r_0}} - 1) = n_0, \quad (6)$$

$$n_e(r_0) e^{-\frac{z a}{r_0}} + \frac{I_e}{4\pi zaD_e} (1 - e^{-\frac{z a}{r_0}}) = n_0. \quad (7)$$

The next step is the definition of r_0 and finding a relation between $I_{i(e)}$ and $n_{i(e)}(r_0)$. Let us put $r_0 = r_{0i} = a + \ell_i$ for the ions and $r_0 = r_{0e} = a + \ell_e$ for the electrons. In the outer region $r > r_0$, we use the drift-diffusion approximation, and the layer $a < r < r_0$ is considered as a collisionless one with a potential of the Coulomb form (3). The ion and electron motions in this layer are determined from the energy and momentum conservation laws. The relation between the ion (electron) flux to the grain from the plasma and the corresponding density at the boundary between the collisionless and hydrodynamic regions $n_{i(e)}(r_{0i(e)})$ was obtained in [9]. In the case of the Maxwellian velocity distribution of ions and electrons in the hydrodynamic region $r > r_0$, it can be written in the form

$$I_i = \pi a^2 n_i(r_{0i}) v_{Ti} \xi_i^{-1}(z) \exp\left(\frac{z\tau a}{r_{0i}}\right), \quad (8)$$

$$I_{ep} = \pi a^2 n_e(r_{0e}) v_{T_e} \xi_e^{-1}(z) \exp\left(-\frac{za}{r_{0e}}\right), \quad (9)$$

where $v_{Ti(e)} = (8T_{i(e)}/\pi m_{i(e)})^{1/2}$ is the ion (electron) thermal velocity, and

$$\xi_i(z) =$$

$$= \begin{cases} \frac{a^2 \exp(za/r_{0i})}{r_{0i}^2 - \ell_i(a + r_{0i}) \exp(za^2/r_{0i}(a + r_{0i}))}, & z < 0, \\ \exp(z\tau), & z \geq 0, \end{cases} \quad (10)$$

$$\xi_e(z) =$$

$$= \begin{cases} \exp(-z), & z \leq 0, \\ \frac{a^2 \exp(-za/r_{0e})}{r_{0e}^2 - \ell_e(a + r_{0e}) \exp(-za^2/r_{0e}(a + r_{0e}))}, & z > 0. \end{cases} \quad (11)$$

The use of the Maxwellian distribution simplifies significantly the expressions for the fluxes $I_{i(e)}$, but, in principle, other distribution functions can be used.

Let us eliminate $n_i(r_{0i})$ from Eqs. (6), (8) and $n_e(r_{0e})$ from Eqs. (7), (9) and take into account that $D_{i(e)} = v_{Ti(e)}\ell_{i(e)}/3$. Then the ion and electron fluxes to the grain are

$$I_i = \frac{4\pi a n_0 z \tau D_i}{\frac{4}{3} z \tau \frac{\ell_i}{a} \xi_i(z) + \exp(za/r_{0i}) - 1}, \quad (12)$$

$$I_{ep} = \frac{4\pi a n_0 z D_e}{\frac{4}{3} z \frac{\ell_e}{a} \xi_e(z) - \exp(-za/r_{0e}) + 1} \times \times \left\{ 1 + \frac{3a}{4z\ell_e} G_{em} \left[1 - \exp\left(-\frac{za}{r_{0e}}\right) \right] \right\}, \quad (13)$$

$$I_e = I_{ep} - I_{em} = \frac{4\pi a n_0 z D_e [1 - G_{em} \xi_e(z)]}{\frac{4}{3} z \frac{\ell_e}{a} \xi_e(z) - \exp(-za/r_{0e}) + 1}, \quad (14)$$

where the dimensionless parameter $G_{em} = I_{em}/\pi a^2 n_0 v_{T_e}$ characterizes the relative intensity of the electron emission without concretization of its mechanism. The parameter G_{em} is simply the ratio of the emitted electron flux density $I_{em}/(4\pi a^2)$ to the thermal electron flux density on a flat surface $n_0 v_{T_e}/4$. The flux balance condition $I_i = I_e$ yields the algebraic equation for the dimensionless grain charge z :

$$\tau \frac{D_i}{D_e} \frac{\frac{4}{3} z \frac{\ell_e}{a} \xi_e(z) - \exp(-za/r_{0e}) + 1}{\frac{4}{3} z \tau \frac{\ell_i}{a} \xi_i(z) + \exp(za/r_{0i}) - 1} = 1 - G_{em} \xi_e(z). \quad (15)$$

Let us consider limiting cases. In the hydrodynamic limit ($\ell_{i(e)}/a \rightarrow 0$), the expressions for the ion and electron fluxes [Eqs. (12) and (14)] reduce to

$$I_i = \frac{4\pi a n_0 z \tau D_i}{e^{z\tau} - 1}, \quad I_e = 4\pi a n_0 z D_e \frac{1 - G_{em} e^{-z}}{1 - e^{-z}}. \quad (16)$$

The dimensionless charge z is determined by

$$\tau \frac{D_i}{D_e} \frac{1 - e^{-z}}{e^{z\tau} - 1} = 1 - G_{em} e^{-z}. \quad (17)$$

These expressions in the absence of electron emission ($G_{em} = 0$) are identical to those derived in [10]. The emission was taken into account in [11], where Eq. (17) was derived for the first time. Note that the parameter G_{em} was determined in [11] in a somewhat different way, namely as $G_{em} = n_e(a)/n_0$. By using (9), (11), and (13), it is easy to show that both definitions coincide in the limit $\ell_{i(e)}/a \rightarrow 0$. Equation (17) yields a particularly simple result in the case of isothermal plasma ($\tau = 1$), $z = \ln(D_i/D_e + G_{em})$.

In the opposite limit of very weak collisionality ($a/\ell_i \rightarrow 0$), we get the equations

$$\frac{e^z - G_{em}}{1 - z\tau} = \frac{v_{T_i}}{v_{T_e}}, \quad z \leq 0, \quad (18)$$

$$e^{z\tau} (1 + z - G_{em}) = \frac{v_{T_i}}{v_{T_e}}, \quad z > 0. \quad (19)$$

In the absence of the electron emission, Eq. (18) coincides with that in the well-known OML approximation (apart from some difference in the determination of z).

Let us put $z = 0$ in Eq. (15) to find the critical value of the parameter G_{em} , at which the grain charge changes the sign. We get

$$G_0 = 1 - \frac{v_{T_i}}{v_{T_e}} \frac{1 + \frac{3a^2}{4\ell_e r_{0e}}}{1 + \frac{3a^2}{4\ell_i r_{0i}}}. \quad (20)$$

When $G_{em} < G_0$, the grain charge is negative, while it is positive in the opposite case. In the limits $\ell_{i(e)}/a \rightarrow 0$ and $a/\ell_{i(e)} \rightarrow 0$, we get $G_0 = 1 - D_i/D_e$ and $G_0 = 1 - v_{T_i}/v_{T_e}$, respectively. Because we always have $v_{T_i} \ll v_{T_e}$ and $D_i \ll D_e$, the second term in Eq. (20) is small, and $G_0 \cong 1$ with a reasonable accuracy.

If the parameter G_{em} is not too small, $G_{em} \gg \tau D_i/D_e$, then the flux balance is shifted significantly as compared that for a non-emitting grain, $G_{em} = 0$. In this case, the left-hand side of Eq. (15) is small and can be omitted. Then

$$G_{em}\xi_e(z) \cong 1. \quad (21)$$

This means physically that the ion flux I_i is small compared to the oppositely directed electron fluxes I_{ep} and I_{em} which practically compensate each other. It is directly seen from Eq. (21) that z is independent of τ , as well as any other characteristic of ions. If $G_{em} < 1$, then $z < 0$ and Eq. (21) reduces to $z = \ln(G_{em})$. Near the critical value ($G_{em} \approx 1$), $|z| \ll 1$, and Eq. (11) yields $\xi_e(z) \approx 1 - z$. Thus, we have $z \approx G_{em} - 1$. Note, that although Eq. (21) does not contain any characteristics of ions, this equation cannot be applied to the purely emissive two-component electron-dust plasma, because the parameter G_{em} is determined in terms of the unperturbed density of electrons and ions n_0 .

3. Screening

The model described in Section 2 is asymptotic in the sense that the screening length λ_D exceeds all characteristic distances in the system and therefore is absent in derived expressions. It was assumed that $\ell_{i(e)}/\lambda_D \rightarrow 0$ and $a/\lambda_D \rightarrow 0$. In the next section, the finiteness of the parameters $\ell_{i(e)}/\lambda_D$ and a/λ_D will be introduced. In order to do this, an explicit form of the potential at large distances is required. Such an asymptotic dependence of $\varphi(r)$ at $r \rightarrow \infty$, when

$$e|\varphi(r)|/T_{i(e)} \ll 1, \quad (22)$$

is determined below.

Let us put $r_0 = \infty$ in Eq. (2) and, consequently, $\varphi(r_0) = 0$, $n_{i(e)}(r_0) = n_0$. Then the flux balance condition $I_i = I_e = I_0$ yields

$$\begin{aligned} n_{i(e)}(r) &= \exp\left(\mp \frac{e\varphi(r)}{T_{i(e)}}\right) \left[n_0 - \right. \\ &\quad \left. - \frac{I_0}{4\pi D_{i(e)}} \int_r^\infty \exp\left(\pm \frac{e\varphi(r')}{T_{i(e)}}\right) \frac{dr'}{r'^2} \right]. \end{aligned} \quad (23)$$

In the region where inequality (22) is satisfied, we have, to within terms on the order of r^{-1} ,

$$n_{i(e)}(r) = n_0 \left(1 \mp \frac{e\varphi(r)}{T_{i(e)}} \right) - \frac{I_0}{4\pi D_{i(e)} r}. \quad (24)$$

Substituting this relation into the Poisson equation, we get

$$\frac{1}{r^2} \frac{d}{dr} \left(r^2 \frac{d\varphi}{dr} \right) = \frac{\varphi}{\lambda_D^2} + \frac{eI_0}{r} \left(\frac{1}{D_i} - \frac{1}{D_e} \right), \quad (25)$$

where $\lambda_D^2 = T_e/4\pi e^2 n_0(1 + \tau)$. The solution of Eq. (25) reads

$$\varphi(r) = \frac{A}{r} e^{-r/\lambda_D} + \frac{eZ_{\text{eff}}}{r}, \quad (26)$$

where A is a constant that can be determined from matching Eq. (26) with the potential at smaller distances (its sign coincides with that of the actual grain charge Z_d), and

$$Z_{\text{eff}} = -I_0 \lambda_D^2 \left(\frac{1}{D_i} - \frac{1}{D_e} \right). \quad (27)$$

Thus, in the region $r \gg \lambda_D$, the electrostatic potential has the Coulomb form

$$\varphi(r) \cong \frac{eZ_{\text{eff}}}{r}. \quad (28)$$

Substituting Eq. (12) into Eq. (27), we get

$$\begin{aligned} z_{\text{eff}} &= \frac{e^2 Z_{\text{eff}}}{T_e a} = -\frac{z\tau}{1 + \tau} \times \\ &\quad \times \frac{1 - \frac{D_i}{D_e}}{\frac{4}{3} z\tau \frac{\ell_i}{a} \xi_i(z) + \exp(z\tau a/(a + \ell_i)) - 1}. \end{aligned} \quad (29)$$

In the limit $\ell_{i(e)} \ll a$, Eq. (29) reduces to

$$\begin{aligned} z_{\text{eff}} &= -\frac{z\tau}{(1 + \tau)(e^{z\tau} - 1)} \left(1 - \frac{D_i}{D_e} \right) \cong \\ &\cong -\frac{z\tau}{(1 + \tau)(e^{z\tau} - 1)} \end{aligned} \quad (30)$$

which coincides with our earlier result [10]. In the opposite limit $\ell_{i(e)} \gg a$, we get

$$z_{\text{eff}} = -\frac{3a}{4\ell_i} \frac{1}{(1 + \tau)\xi_i(z)} \left(1 - \frac{D_i}{D_e} \right),$$

$$\xi_i(z) = \begin{cases} (1 - z\tau)^{-1}, & z \leq 0, \\ e^{z\tau}, & z > 0. \end{cases} \quad (31)$$

Consequently, $z_{\text{eff}} \rightarrow 0$ as $a/\ell_i \rightarrow 0$. This result is in agreement with the known behavior of the electrostatic potential $\varphi(r) \sim r^{-2}$ in the fully collisionless regime [12]. However, the direct transition to this dependence is impossible because of the condition $\ell_i \ll \lambda_D$.

It is easy to show that $z_{\text{eff}} < 0$ independently of the sign of the charge z . Even for an uncharge grain (when $G_{em} = G_0$), its effective charge is negative and finite:

$$z_{\text{eff}}|_{z=0} = -\frac{1 - \frac{D_i}{D_e}}{(1 + \tau) \left(\frac{4\ell_i}{3a} + \frac{a}{a + \ell_i} \right)}. \quad (32)$$

The negativity of the effective charge of a grain is obvious already from Eq. (27), because $I_0 > 0$ and $D_e > D_i$.

Thus, for $Z_d < 0$, the grain charge is not fully screened, while, for $Z_d > 0$, the overscreening of the grain charge occurs, and the electrostatic potential (26) changes its sign at a certain distance. In the context of the pair particle interaction potential, this implies a long-range attractive asymptote of the electrostatic interaction potential. This attraction was previously obtained numerically [13] and analytically by means of the plasma linear response formalism [14]. The location of the potential minimum r_{\min} can be found by solving the equation

$$\left(1 + \frac{r}{\lambda_D}\right) \exp\left(-\frac{r}{\lambda_D}\right) = \frac{e|Z_{\text{eff}}|}{A}. \quad (33)$$

The potential depth is

$$|\varphi(r_{\min})| = \frac{e|Z_{\text{eff}}|}{\lambda_D + r_{\min}}. \quad (34)$$

4. Accounting for the Finiteness of the Screening Length

The charging model developed in Section 2 does not contain the dependence of the grain charge on the screening length. To account for this dependence, let us approximate the potential $\varphi(r)$ combining Eqs. (3) and (28) by the function

$$\varphi(r) = \begin{cases} \frac{eZ_d}{r} + \varphi_c, & r < a + \lambda_D, \\ \frac{eZ_{\text{eff}}}{r}, & r \geq a + \lambda_D. \end{cases} \quad (35)$$

Such an approximation allows the analytic integration in Eqs. (2). The continuity condition at $r = a + \lambda_D$ results in

$$\varphi_c = -\frac{e(Z_d - Z_{\text{eff}})}{a + \lambda_D}. \quad (36)$$

Then, we follow the procedure described in Section 2 but without the restriction $r < r_1$, because potential (35) is specified within the whole range of r . Therefore, the passage from Eqs. (4), (5) to Eqs. (6), (7) occurs at $r \rightarrow \infty$. As a result, the expressions for the ion and electron fluxes to a grain are

$$I_i = \frac{4\pi a n_0 z \tau D_i}{Q_i(z, y)}, \quad (37)$$

$$I_e = I_{ep} - I_{em} = \frac{4\pi a n_0 z D_e}{Q_e(z, y)} \times$$

$$\times \left[1 - G_{em} \xi_e(z) \exp\left(z(1-y) \frac{a}{a + \lambda_D}\right) \right], \quad (38)$$

where $y = z_{\text{eff}}/z$, and

$$\begin{aligned} Q_i(z, y) = & \frac{4}{3} z \tau \frac{\ell_i}{a} \xi_i(z) \exp\left[-z\tau(1-y) \frac{a}{a + \lambda_D}\right] + \\ & + \exp\left[z\tau a \left(\frac{1}{r_{0i}} - \frac{1-y}{a + \lambda_D}\right)\right] + \\ & + \left(\frac{1}{y} - 1\right) \exp\left(z\tau y \frac{a}{a + \lambda_D}\right) - \frac{1}{y}, \end{aligned} \quad (39)$$

$$\begin{aligned} Q_e(z, y) = & \frac{4}{3} z \frac{\ell_e}{a} \xi_e(z) \exp\left[z(1-y) \frac{a}{a + \lambda_D}\right] - \\ & - \exp\left[-za \left(\frac{1}{r_{0e}} - \frac{1-y}{a + \lambda_D}\right)\right] - \\ & - \left(\frac{1}{y} - 1\right) \exp\left(-zy \frac{a}{a + \lambda_D}\right) + \frac{1}{y}. \end{aligned} \quad (40)$$

The first equation connecting two independent variables z and y follows from the flux balance conditions:

$$\tau \frac{D_i}{D_e} \frac{Q_e(z, y)}{Q_i(z, y)} = 1 - G_{em} \xi_e(z) \exp\left[z(1-y) \frac{a}{a + \lambda_D}\right]. \quad (41)$$

The second equation is obtained by the substitution of Eq. (37) or (38) in Eq. (27). Using Eq. (37), we get

$$y Q_i(z, y) = -\frac{\tau}{1 + \tau} \left(1 - \frac{D_i}{D_e}\right). \quad (42)$$

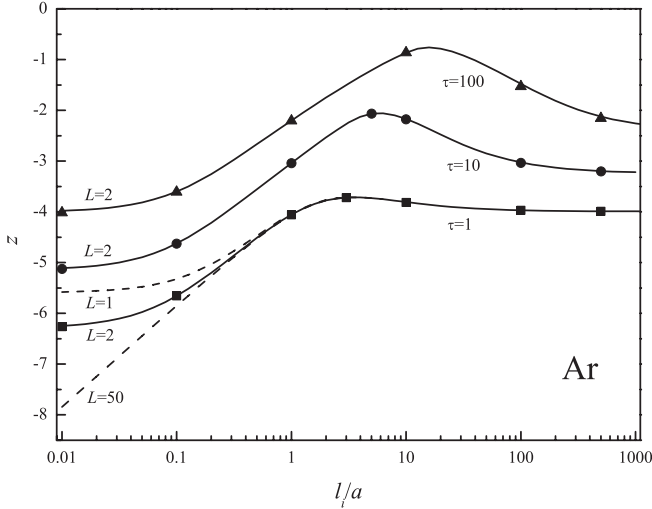


Fig. 1. Dimensionless grain charge z as a function of the ion mean free path ℓ_i normalized to the grain radius a in argon plasmas in the absence of the electron emission ($G_{em} = 0$) for various values of $\tau = T_e/T_i$ and $L = \ell_e/\ell_i$. Curves correspond to the solution of Eq. (15), points are the result of numerical calculations

The actual Z_d and effective Z_{eff} grain charges are found from solutions of the system of equations (41) and (42). Unlike the asymptotic model, where Z_d is determined by the solution of Eq. (15) independently of Z_{eff} and only then the effective charge is calculated with the help of Eq. (29), both charges are determined here simultaneously. It is quite natural, because Z_d depends on the behavior of the potential in the asymptotic region.

In the limit $a/\lambda_D \rightarrow 0$, Eqs. (41) and (42) are uncoupled, and the transition to the asymptotic model is realized. In this case, Eq. (41) reduces to Eq. (15) and Eq. (42) reduces to Eq. (29). In the hydrodynamic limit $\ell_{i(e)}/a \rightarrow 0$, functions (39), (40), and ξ_e become simpler, but the system of equations (41) and (42) has the same form.

The critical value G_0 of the parameter G_{em} remains unchanged in comparison with the asymptotic model. Equation (20) remains valid, as well as the corresponding expression for the effective charge (32). It is easy to write an analog of Eq. (21) corresponding to the approximate balance of the electron fluxes I_{ep} and I_{em} provided that the ion flux I_i (equal to their small difference) is neglected. Thus, it is done by replacing the left-hand side of Eq. (41) by zero. The substitution of its solution $y = 1 + (a + \lambda_D) \ln[G_{em} \xi_e(z)]/za$ in Eq. (42) reduces the problem to find z to the solution of one equation.

5. Comparison of Results with Those of Numerical Calculations

Besides the developed analytical model, numerical calculations were performed as well. We have solved the system of differential equations consisting of Eqs. (1) for ions and electrons and the Poisson equation written in the form

$$\frac{dZ}{dr} = 4\pi r^2(n_i - n_e), \quad (43)$$

where $Z = Z(r)$ is the charge inside a sphere of radius r . The boundary conditions at $r = r_0$ for Eqs. (1) are relations (8) and (9), and one for Eq. (43) is $Z(r_0) = Z_d$ (since $r_0 \ll \lambda_D$). All these equations are of the first order, thus these boundary conditions constitute formally a complete set. However, they depend on the beforehand unknown values Z_d , I_i , and I_{ep} . Thus, additional conditions are necessary. As those, we use $n_i = n_e$ and $dZ/dr = 0$ as $r \rightarrow \infty$.

The dimensionless grain charge z as a function of the ion mean free path ℓ_i normalized to the grain radius a in argon plasmas in the absence of the electron emission ($G_{em} = 0$) for different values of $\tau = T_e/T_i = 1, 10, 100$ and $L = \ell_e/\ell_i = 1, 2, 50$ is shown in Fig. 1. Curves correspond to the solution of the algebraic equation (15), points are the result of numerical calculations. A smooth transition from the pure hydrodynamic regime with small mean free path (the left side of the figure) to the regime with a thick Knudsen layer (the right side of the figure) takes place. The grain charge is always negative. An increase in τ results in a decrease in $|z|$ at all values of the parameter ℓ_i/a . The weakly pronounced maximum of the function $z(\ell_i/a)$ at $\tau = 1$ becomes more visible for larger τ and shifts in the direction of higher values of the argument. The parameter L affects the grain charge only at small values of ℓ_i/a . For other gases, such as hydrogen, helium, neon, and xenon, the dependence of z on τ , L , and ℓ_i/a is qualitatively the same. As seen from Fig. 1, there is a good agreement between the results of the analytical model and numerical calculations.

Our calculations showed that the accounting of a Knudsen layer in the hydrodynamic approximation results in a decrease in the absolute value of negative grain charge. This decrease can be rather large, about two times for isothermal plasma ($\tau = 1$) and five times at $\tau = 100$.

The ratio of effective and actual grain charges Z_{eff}/Z_d as a function of the screening length λ_D normalized to the grain radius a in argon plasmas is shown in Fig. 2. The results of the analytical model are compared with our numerical calculation and with a

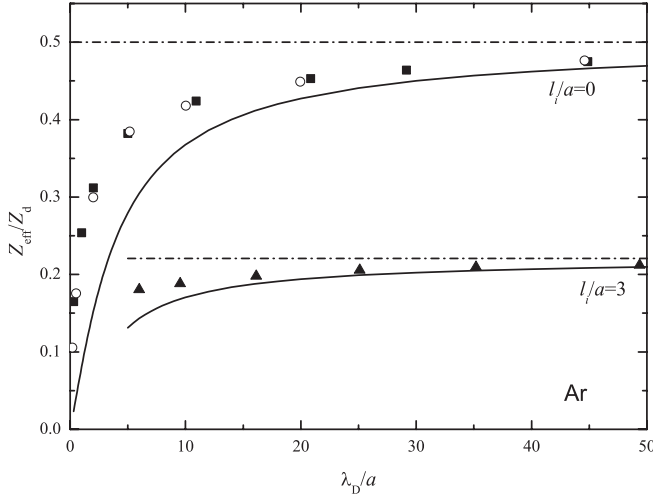


Fig. 2. Ratio of effective and actual grain charges Z_{eff}/Z_d as a function of the screening length λ_D normalized to the grain radius a in argon plasmas at $G_{\text{em}} = 0$, $\tau = 1$, $L = 2$ and $\ell_i/a = 0, 3$. Solid curves correspond to the analytic model solution of the system of equations (39) and (40); dash-dotted curves correspond to the asymptotic model ($\lambda_D/a \rightarrow \infty$); and symbols correspond to the numerical calculations of the present work (filled) and [7] (open)

numerical solution by Bystrenko and Zagorodny [7] who used the hydrodynamic approximation with boundary conditions at the grain surface (this corresponds to $\ell_i/a \rightarrow 0$ in our model). The results of numerical calculations obtained by different methods practically coincide. The ratio Z_{eff}/Z_d derived from the asymptotic model slightly underestimate the numerical values.

Let us consider now the influence of the electron emission. Figure 3 shows how the parameter λ_D/a affects the dependence of z on G_{em} . In all cases, decreasing λ_D/a results in increasing $|z|$, for both positive and negative z . At the same time, the grain charge remains practically independent of the parameters other than G_{em} in the region $0.1 < G_{\text{em}} < 2$. Decreasing the parameter λ_D/a strongly affects the value of z at larger values of G_{em} and ℓ_i/a . At small ℓ_i/a (curves corresponding to $\ell_i/a = 0$ in Fig. 3), z only weakly depends on λ_D/a at all G_{em} . But, for $\ell_i/a = 2$, this dependence becomes rather strong for $G_{\text{em}} \gtrsim 10$.

The dependence of z on λ_D/a at various intensities of the electron emission in the limiting case of perfect hydrodynamics, $\ell_i/a = 0$, is shown in Fig. 4. The case of a significant thickness of the Knudsen layer $\ell_i/a = 2$ is presented in Fig. 5. In these figures, the results of numerical calculations are shown as well. At $\lambda_D/a \gg 1$, the grain charge is close to the value corresponding to

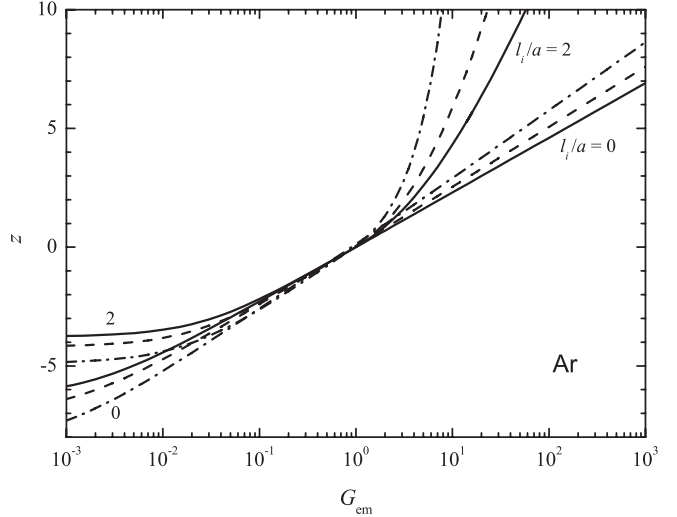


Fig. 3. Dimensionless grain charge z as a function of the emissivity G_{em} in argon plasmas for $\tau = 1$, $L = 2$, and $\ell_i/a = 0, 2$. Solid curves correspond to $\lambda_D/a \rightarrow \infty$, dashed curves correspond to $\lambda_D/a = 10$, and dash-dotted curves correspond to $\lambda_D/a = 4$

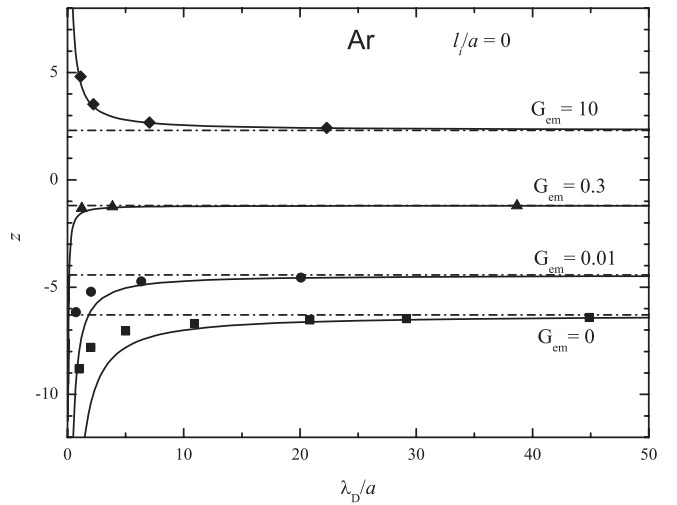


Fig. 4. Dimensionless grain charge z as a function of λ_D/a in argon plasmas for $\tau = 1$, $L = 2$, $\ell_i/a = 0$, and $G_{\text{em}} = 0, 0.01, 0.3, 10$. Solid curves correspond to the analytical model, dash-dotted curves correspond to the asymptotic solution $\lambda_D/a \rightarrow \infty$, and symbols correspond to the numerical calculation

the asymptotic model (dash-dotted curves). At $\lambda_D/a \sim 1$, the deviations from the asymptotic model are very significant, the magnitude of these deviations in the numerical calculation being smaller than that in the analytical model. A similar situation takes place for the effective charge (see Fig. 6).

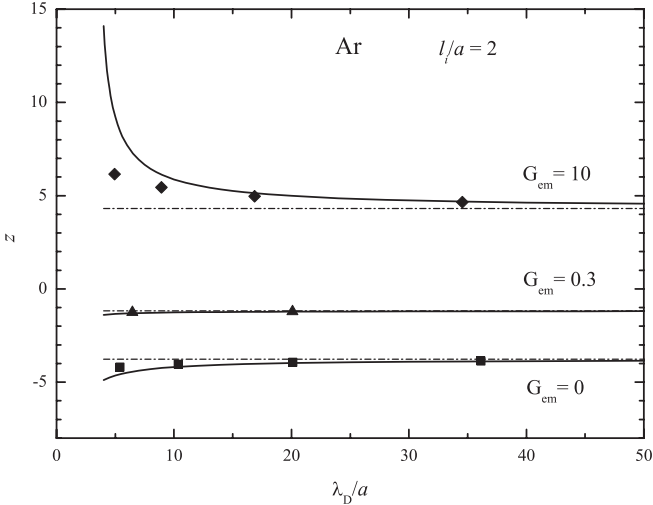


Fig. 5. Dimensionless grain charge z as a function of λ_D/a in argon plasmas for $\tau = 1$, $L = 2$, $\ell_i/a = 2$, and $G_{em} = 0, 0.3, 10$. Solid curves correspond to the analytical model, dash-dotted curves correspond to the asymptotic solution $\lambda_D/a \rightarrow \infty$, and symbols correspond to the numerical calculation

6. Conclusions

We have proposed a model of dust grain charging in a weakly ionized plasma in the hydrodynamic approximation. We considered the conditions when the grain radius a and the mean free paths of ions ℓ_i and electrons ℓ_e are of the same order, and the collisionless (Knudsen) layer around a grain should be taken into account. It is assumed that the processes of volume ionization and recombination in the plasma region perturbed by the grain are not important and do not affect the value of the ion and electron fluxes to the grain. The screening length λ_D is assumed large in comparison with the grain radius and the mean free paths of ions and electrons. The expressions for the ion and electron fluxes to a grain and the algebraic equation for its charge Z_d are obtained. Changes in the grain charge during the transition from a thin to a thick collisionless layer around the grain are traced. The model also allows one to account for the electron emission from the grain surface. The electron emission (secondary, thermo-, or photoemission) reduces the absolute magnitude of the grain charge, and it becomes positive at sufficiently large emission intensities. The dimensionless parameter which characterizes the electron emission intensity is introduced, and the criterion of a change of the particle charge sign is given. We have considered the behavior of the electrostatic potential at large distances from

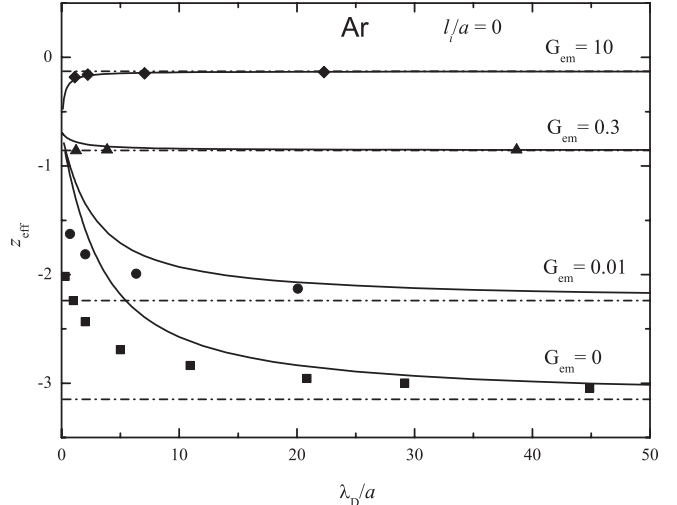


Fig. 6. Dimensionless effective grain charge z_{eff} as a function of λ_D/a in argon plasmas for $\tau = 1$, $L = 2$, $\ell_i/a = 0$, and $G_{em} = 0, 0.01, 0.3, 10$. Solid curves correspond to the analytical model, dash-dotted curves correspond to the asymptotic solution $\lambda_D/a \rightarrow \infty$, and symbols correspond to the numerical calculation

the grain and shown that it has the Coulomb-like form with some effective charge Z_{eff} . The effective charge is always negative independently of the sign of the actual charge Z_d . This implies that, for a negatively charged grain, only the partial screening occurs; whereas, for a positively charged grain, the potential reverses its sign at some point and becomes negative. In the latter case, the electrostatic attraction is possible between a pair of positively charged grains.

We would like to thank A.V. Filippov for the helpful discussions. L.G.D. and A.G.K. are supported by the Program of researches of matter under extreme conditions of the Presidium of the Russian Academy of Sciences and the Russian Foundation for Basic Research through Grants No. 06-02-08100 and No. 08-02-00444. S.A.K. is supported by DLR under Grant N 50WP0203.

1. V.E. Fortov, A.G. Khrapak, S.A. Khrapak *et al.*, Phys. Usp. **47**, 447 (2004).
2. V.E. Fortov, A.V. Ivlev, S.A. Khrapak *et al.*, Phys. Reports **421**, 1 (2005).
3. S.A. Khrapak, S.V. Ratynskaya, A.V. Zobnin *et al.*, Phys. Rev. E **72**, 016406 (2005).
4. A.F. Pal', A.O. Serov, A.N. Starostin *et al.*, JETP **92**, 235 (2001).
5. A.F. Pal', D.V. Sivokhin, A.N. Starostin *et al.*, Plasma Phys. Rep. **28**, 28 (2002).
6. A.V. Filippov, N.A. Dyatko, A.F. Pal', and A.N. Starostin, Plasma Phys. Rep. **29**, 190 (2003).

7. O. Bystrenko, A. Zagorodny, Phys. Rev. E **67**, 066403 (2003).
8. C.H. Su, S.H. Lam, Phys. Fluids **6**, 1479 (1963).
9. L.G. D'yachkov, A.G. Khrapak, J. Phys. A **39**, 4561 (2006).
10. S.A. Khrapak, G.E.Morfill, A.G.Khrapak, and L.G. D'yachkov, Phys. Plasmas **13**, 052114 (2006).
11. L.G. D'yachkov, A.G. Khrapak, S.A. Khrapak, JETP **106**, 166 (2008).
12. Y.L. Al'pert, A.V. Gurevich, and L.P. Pitaevskii, *Space Physics with Artificial Satellites* (Consultant Bureau, New York, 1965).
13. A.V. Filippov, A.F. Pal, and A.N. Starostin, in *Proceed. 2nd Int. Confer. "Dusty Plasmas in Applications"* (August 26–30, 2007, Odesa, Ukraine), p. 44.
14. S.A. Khrapak, G.E. Morfill, V.E. Fortov et al., Phys. Rev. Lett. **99**, 055003 (2007).

Received 31.10.07

ГІДРОДИНАМІЧНЕ НАБЛИЖЕННЯ ДЛЯ ЗАРЯДЖАННЯ ПОРОШИНКОВ СЛАБКОІОНІЗОВАНІЙ ПЛАЗМІ

Л.Г. Д'ячков, С.А. Храпак, А.Г. Храпак

Р е з ю м е

Досліджено вплив як кнудсенівського (без зіткнень) шару поблизу порошинки у плазмі, так і емісії електронів з поверхні порошинки на її заряд та екронування. Вважається, що іонізація і рекомбінація поблизу порошинки відсутні. Отримано критерій для зміни знака заряду порошинки. Показано, що електростатичний потенціал на асимптотично великих відстанях поводиться як кулонівський потенціал ефективного заряду Z_{eff} , який завжди негативний незалежно від знака фактичного заряду Z_d . Для $Z_d > 0$ електростатичний потенціал змінює знак і має мінімум, що свідчить про можливість існування електростатичного притягання між позитивно зарядженими порошинками.